Optical recording of electrical activity in intact neuronal networks with random access second-harmonic generation microscopy

Leonardo Sacconi,[1,2,*] Jonathan Mapelli,[3] Daniela Gandolfi,[3] Jacopo Lotti,[1] Rodney P. O'Connor,[1] Egidio D'Angelo[3] and Francesco S. Pavone[1,2]

[1] European Laboratory for Nonlinear Spectroscopy (LENS), University of Florence, Italy
[2] Department of Physics, University of Florence, Italy
[3] Department of Cellular-Molecular Physiological and Pharmacological Sciences, University of Pavia, Italy
*Corresponding author: sacconi@lens.unifi.it

Abstract: One of the main challenges in understanding the central nervous system is to measure the network dynamics of neuronal assemblies, while preserving the computational role of individual neurons. However, this is not possible with current techniques. In this work, we combined the advantages of second-harmonic generation (SHG) with a random access (RA) excitation scheme to realize a new microscope (RASH) capable of optically recording fast membrane potential events occurring in a wide-field of view. The RASH microscope, in combination with bulk loading of tissue with FM4-64 dye, was used to simultaneously record electrical activity from clusters of Purkinje cells in acute cerebellar slices. Complex spikes, both synchronous and asynchronous, were optically recorded simultaneously across a given population of neurons. Spontaneous electrical activity was also monitored simultaneously in pairs of neurons, where action potentials were recorded without averaging across trials. These results show the strength of this technique in describing the temporal dynamics of neuronal assemblies, opening promising perspectives in understanding the computations of neuronal networks.

OCIS codes: (180.4315) Nonlinear microscopy; (170.1420) Biology.

References and links

1. A. Grinvald and R. Hildesheim, "VSDI: a new era in functional imaging of cortical dynamics," Nat. Rev. Neurosci. **5**, 874-885 (2004).
2. M. Zochowski, M. Wachowiak, C. X. Falk, L. B. Cohen, Y. W. Lam, S. Antic, and D. Zecevic, "Imaging membrane potential with voltage-sensitive dyes," Biol. Bull. **198**, 1-21 (2000).
3. S. D. Antic, "Action potentials in basal and oblique dendrites of rat neocortical pyramidal neurons," J. Physiol. **550**, 35-50 (2003).
4. J. E. Gonzalez and R. Y. Tsien, "Improved indicators of cell membrane potential that use fluorescence resonance energy transfer," Chem. Biol. **4**, 269-277 (1997).
5. T. Knopfel, K. Tomita, R. Shimazaki, and R. Sakai, "Optical recordings of membrane potential using genetically targeted voltage-sensitive fluorescent proteins," Methods **30**, 42-48 (2003).
6. M. S. Siegel and E. Y. Isacoff, "A genetically encoded optical probe of membrane voltage," Neuron **19**, 735-741 (1997).
7. R. A. Stepnoski, A. LaPorta, F. Raccuia-Behling, G. E. Blonder, R. E. Slusher, and D. Kleinfeld, "Noninvasive detection of changes in membrane potential in cultured neurons by light scattering," Proc. Natl. Acad. Sci. U S A **88**, 9382-9386 (1991).
8. F. Helmchen and W. Denk, "Deep tissue two-photon microscopy," Nat. Methods **2**, 932-940 (2005).
9. W. R. Zipfel, R. M. Williams, and W. W. Webb, "Nonlinear magic: multiphoton microscopy in the biosciences" Nat. Biotechnol. **21**, 1369-1377 (2003).
10. J. A. Fisher, J. R. Barchi, C. G. Welle, G. H. Kim, P. Kosterin, A. L. Obaid, A. G. Yodh, D. Contreras, and B. M. Salzberg, "Two-photon excitation of potentiometric probes enables optical recording of action potentials from mammalian nerve terminals in situ," J. Neurophysiol. **99**, 1545-53 (2008).

11. P. J. Campagnola and L. M. Loew, "Second-harmonic imaging microscopy for visualizing biomolecular arrays in cells, tissues and organisms," Nat. Biotechnol. **21**, 1356-60 (2003).
12. L. Moreaux, O. Sandre, M. Blanchard-Desce, and J. Mertz, "Membrane imaging by simultaneous second harmonic generation and two photon microscopy," Opt. Lett. **25**, 320–322 (2000).
13. O. Bouevitch, A. Lewis, I. Pinevsky, J. P. Wuskell, and L. M. Loew, "Probing membrane potential with non-linear optics," Biophys. J. **65**, 672–679 (1993).
14. T. Pons, L. Moreaux, O. Mongin, M. Blanchard-Desce, and J. Mertz, "Mechanics of membrane potential sensing with second-harmonic generation micrsocopy," J. Biomed. Opt. **8**, 428-431 (2003).
15. D. A. Dombeck, M. Blanchard-Desce, and W. W. Webb, "Optical recording of action potentials with second-harmonic generation microscopy," J. Neurosci. **24**, 999-1003 (2004).
16. L. Sacconi, D. A. Dombeck, and W. W. Webb, "Overcoming photodamage in second-harmonic generation microscopy: real-time optical recording of neuronal action potentials," Proc. Natl. Acad. Sci. U S A **103**, 3124-3129 (2006).
17. D. A. Dombeck, L. Sacconi, M. Blanchard-Desce, and W. W. Webb, "Optical recording of fast neuronal membrane potential transients in acute mammalian brain slices by second-harmonic generation microscopy," J. Neurophysiol. **94**: 3628-3636 (2005).
18. M. Nuriya, J. Jiang , B. Nemet, K. B. Eisenthal, and R. Yuste, "Imaging membrane potential in dendritic spines," Proc. Natl. Acad. Sci. U S A **103**, 786-790 (2006).
19. A. Bullen, S. S. Patel, and P. Saggau, "High-speed, random-access fluorescence microscopy: I. High-resolution optical recording with voltage-sensitive dyes and ion indicators," Biophys. J. **73**, 477-491 (1997).
20. R. Salome, Y. Kremer, S. Dieudonne, J. F. Leger, O. Krichevsky, C. Wyart, D. Chatenay, and L. Bourdieu, "Ultrafast random-access scanning in two-photon microscopy using acousto-optic deflectors," J. Neurosci. Methods **154**, 161-174 (2006).
21. V. Iyer, T. M. Hoogland, and P. Saggau, "Fast functional imaging of single neurons using random-access multiphoton (RAMP) microscopy," J. Neurophysiol. **95**, 535-545 (2006).
22. J. C. Eccles, "The cerebellum as a computer: patterns in space and time," J. Physiol. **229**, 1–32 (1969).
23. D. Marr, "A theory of cerebellar cortex," J. Physiol. **202**: 437-470 (1969).
24. J. Mapelli and E. D'Angelo, "The spatial organization of long-term synaptic plasticity at the input stage of cerebellum. J. Neurosci. **27**, 1285-1296 (2007).
25. R. Llinas and M. Sugimori, "Electrophysiological properties of in vitro Purkinje cell dendrites in mammalian cerebellar slices," J. Physiol. **305**, 197-213 (1980).
26. R. Llinas and M. Sugimori, "Electrophysiological properties of in vitro Purkinje cell somata in mammalian cerebellar slices," J. Physiol. **305**, 171-195 (1980).
27. L. Moreaux, O. Sandre, M. Blanchard-Desce, and J. Mertz, "Membrane imaging by simultaneous second-harmonic generation and two-photon microscopy," Opt. Lett. **25**, 320-322 (2000).
28. S. L.Palay and V. Chan-Palay, "Cerebellar Cortex: Cytology and organization," Berlin: Springer-Verlag (1974).
29. J. C. Eccles, M. Ito, and J. Szentagothai, "The cerebellum as a neuronal machine," Berlin: Springer.-Verlag (1967).
30. H. Nishiyama and D. J. Linden, "Differential maturation of climbing fiber innervation in cerebellar vermis," J. Neurosci. **24**, 3926-3932 (2004).
31. T. Z. Teisseyre, A. C. Millard, P. Yan, J. P. Wuskell, M. D. Wei, A. Lewis, and L. M. Loew , "Nonlinear optical potentiometric dyes optimized for imaging with 1064-nm light," J. Biomed .Opt. **12**, 044001 (2007).
32. N. Ji, J. C. Magee, and E. Betzig, "High-speed, low-photodamage nonlinear imaging using passive pulse splitters," Nat. Methods **5**, 197-202 (2008).
33. U. Egert, D. Heck, and A. Aertsen, "Two-dimensional monitoring of spiking networks in acute brain slices," Exp. Brain Res. **142**, 268-274 (2002).
34. G. D. Reddy and P. Saggau, "Fast three-dimensional laser scanning scheme using acousto-optic deflectors," J. Biomed. Opt. **10**, 064038 (2005).
35. S. Shoham, D. H. O'Connor, and R. Segev, "How silent is the brain: is there a "dark matter" problem in neuroscience?," J. Comp. Physiol. A Neuropathol. Sens. Neural Behav. Physiol. **192**, 777-784 (2006).
36. V. Nikolenko, K. E. Poskanzer, and R. Yuste, "Two-photon photostimulation and imaging of neural circuits,". Nat. Methods **4**, 943-950 (2007).
37. E. S. Boyden, F. Zhang, E. Bamberg, G. Nagel, and K. Deisseroth, "Millisecond-timescale, genetically targeted optical control of neural activity," Nat. Neurosci. **8**, 1263-1268 (2005).

1. Introduction

The central nervous system can process a tremendous amount of information, which is encoded in terms of spikes and transmitted between neurons at synapses. A central question in

neuroscience is how simple processes in neurons can generate cognitive functions and form complex memories like those experienced by humans and animals. In principle, if one were able to record from all the neurons in a network involved in a given behavior, it would be possible to reconstruct the related computations. Unfortunately, this is not possible with current techniques for several reasons. Generally, the more precise the method of neuronal recording is (e.g. patch-clamp), the more limited the number of simultaneously recorded neurons becomes. Conversely, global recordings (e.g. field recordings) collect activity from many neurons but lose information about the computation of single neurons.

Current optical techniques for recording membrane potential (Vm) can potentially overcome these problems [1,2]. Most approaches to the optical recording of fast Vm events in neural systems rely on one-photon methods [3-7]. These methods can be used to generate high signal-to-noise ratio (S/N) measurements of action potentials (APs) from sub-cellular regions in a single trial and sub-threshold events with averaging. However, in intact tissue slices their effectiveness in detecting AP in multiple deep neurons is markedly limited because strong multiple light scattering blurs the images. In order to record deep Vm activity in intact systems maintaining a high spatial resolution, nonlinear optical methods, such as two-photon fluorescence and second-harmonic generation (SHG) are needed [8-11]. Since dye molecules not embedded in the plasma membrane are randomly oriented and do not contribute to the SHG signal, this technique is advantageous for high-contrast imaging of membranes [12]. The possibility of using SHG to report the amplitude of the electrical potential across a membrane was first demonstrated on model membranes by Loew and colleagues [13]. Recently, fast (~ 1 ms) SHG recordings of Vm have been achieved in model membranes [14], in Aplysia neurons in culture [15,16] and in intact mammalian neural systems [17,18]. The next challenge is to record multiple APs simultaneously from multiple neurons in intact systems.

In this regard, the major limiting factor of non-linear microscopes is their scanning time. For this reason, the optical recording of neuronal APs is possible only in a single position of the neuron by using a line scanning procedure [15]. In principle, the optical measurement of time-dependent processes does not require the production of images at all. Instead, more time should be spent collecting as many photons as possible from selective positions, where the image plane intersects the biological objects of interest. Using this approach, fast physiological processes, like APs in the soma of multiple neurons, can be recorded at a sampling frequency of more than 1 kHz. This cannot be achieved with a standard galvanometer mirror since about 1 ms is the time required to reach and stabilize a new position. Scanning a set of points within a plane at high speed is possible with two orthogonal acousto-optic deflectors (AODs). In an AOD, a propagating ultrasonic wave establishes a grating that diffracts a laser beam at a precise angle which can be changed within a few microseconds. The first implementation of a high-speed, random-access, laser-scanning fluorescence microscope configured to record fast physiological signals from small neuronal structures with high spatiotemporal resolution has been presented by Bullen et al. [19]. Recently, two-photon microscopy using AODs was used also to perform fast calcium imaging in cultured neurons [20] and in brain slices [21].

In this work, we combined the advantages of SHG with an AOD-based random access (RA) laser excitation scheme to produce a new microscope (RASH) capable of optically recording fast Vm events (~ 1 ms). This system is capable of resolving APs occurring simultaneously in several neurons in a wide-field (150 × 150 μm^2) configuration, and with deep tissue penetration in living brain slices. The multiple single-neuron electrical recording was performed in the Purkinje cell layer of the cerebellum [22,23]. Acute cerebellar slices were used and labeled by bulk loading of the styryl dye FM4-64. This staining procedure allowed large-scale SHG imaging without causing any perturbations to the electrophysiological properties of the neurons. The RASH microscope was used, in combination with patch-clamp techniques, to detect complex spikes and simple spikes, demonstrating the capability of this system to optically record single APs in a cluster of Purkinje cells (PCs) simultaneously. These results show that the RASH microscope provides a

new powerful tool for investigating neural circuit activity by simultaneously monitoring APs in arbitrarily selected multiple single neurons.

2. Materials and Methods

2.1 Slice preparation and staining

Acute cerebellar slices (200 µm thick) were obtained from 18- to 25-d-old Wistar rats. Rats were anesthetized with Halothane (0.5 ml in 2 L for 1–2 min) before being killed by decapitation. The cerebellum was gently removed, and the vermis was isolated, fixed on a support with cyanoacrylate glue, and immersed into a cold (2-3 °C) cutting solution. Slices were cut in the sagittal plane. The cutting solution contained the following (in mM): 130 K-gluconate, 15 KCl, 0.2 EGTA, 20 HEPES, 10 glucose, pH 7.4 with NaOH. Slices were incubated for ≈ 1 h at 32 °C before recordings at room temperature in oxygenated Krebs' solution containing the following (in mM): 120 NaCl, 2 KCl, 1.2 $MgSO_4$, 26 $NaHCO_3$, 1.2 KH_2PO_4, 2 $CaCl_2$, 11 glucose, pH 7.4 when equilibrated with 95% O_2 – 5% CO_2. The bulk loading was performed by incubating the slice for ≈ 30 min at room temperature in 1 mL of oxygenated Krebs' solution containing 100 µg of FM4-64 dye (T13320, Invitrogen). Slices were gently positioned on the recording chamber and fixed with a nylon mesh attached to platinum Ω-wire to improve tissue adhesion and mechanical stability. Perfusion of oxygenated Krebs' solution was continued during the recording session. Slices were used soon after incubation to limit potential time-dependent effects deriving from progressive tissue damage.

2.2 Electrophysiology

Whole cell patch-clamp recordings were obtained under infrared video microscopy using an Axoclamp 2b amplifier (Axon Instruments). During whole cell recording, the pipettes were filled with intracellular solution containing (in mM) 145 K-Gluconate, 10 HEPES, 0.2 EGTA, 4.6 $MgCl_2$, 5 KCl, 4 ATP-Na_2, 0.4 GTP-Na (pH 7.4 with KOH). The pipette resistance was 3-4 MΩ. Once a GΩ seal was obtained, quick negative pressure pulses opened the seal for recording. In cell attached recording the pipettes were filled with Krebs' solution and a 50 MΩ seal was achieved before monitoring current. The patch-clamp amplifier was controlled by a pc using custom-made software developed in LabVIEW 7.1 (National Instruments).

Bipolar tungsten electrodes (100 µm tips separated by 250 µm, impedance 500 KΩ) were used to stimulate the climbing fibers. The bipolar electrode was placed across axial fiber bundle in the cerebellar lamina and was driven by a custom made electrical stimulator providing a pulse of 5-20 V in amplitude and 200 µs of duration time.

2.3 Random access second-harmonic generation (RASH) microscope

The RASH is comprised of a custom-made upright scanning microscope (see Fig. 1). The excitation was provided by a high power, passively mode-locked fiber laser operating in the 1064 nm spectral range (FP1060-2s, Fianium). We used this excitation light because, in combination with FM4-64 dye, it currently appears to be the most promising excitation wavelength for fast optical recording of Vm in intact preparations [17]. The scanning head was developed by using an acousto-optical deflection (AOD) system comprised of two AODs crossed at 90° (DTSXY-250-1064, AA opto-electronic). The spatial distortion of the laser pulse in the AODs is known to affect the radial and axial resolutions of the microscope. To compensate for the larger dispersion due to two crossed AODs, we used an acousto-optical modulator (AOM) placed at 45° with respect to the two axes of the AODs (see Fig. 1). We chose the appropriate propagation direction and frequency of the ultrasonic wave in the AOM, which propagates in the opposite direction with respect to the sum of the two waves in the AODs. In order to compensate for the spatial distortion at the center of the field of view (F0), its frequency was fixed at a value given by F0·$\sqrt{2}$ (see reference [20] for more details). A microscope objective XLUM 20×, NA 0.95, WD 2 mm (Olympus) was used to focus the excitation light in the tissue. The SHG signal was collected in the forward direction. Since the

excitation beam is focused by a high-numerical aperture objective, the resulting SHG signal is dominantly emitted off-axis and the collector condenser was chosen with an appropriate numerical aperture (NA 1.4, Olympus) to collect the entire SHG signal. The SHG was detected with a GaAsP photomultiplier module (H7422, Hamamatsu) after blocking both transmitted laser light and concurrent two-photon excited fluorescence with a band-pass filter (FF01-531/22-50.8-D, Semrock). All the microscope optics were fixed onto a custom vertical honeycomb steel breadboard. The opto-electronic components of the setup were computer-controlled with custom-made software developed in LabVIEW 7.1 (National Instruments). The RASH microscope was capable of collecting a field of view of 150×150 μm^2 with a radial spatial resolution of ~ 800 nm. The commutation time between two positions in the focal plane is of the order of 4 μs. For all experiments the laser power was 10 - 20 mW, as measured after the objective lens and depended on the depth of the chosen plane.
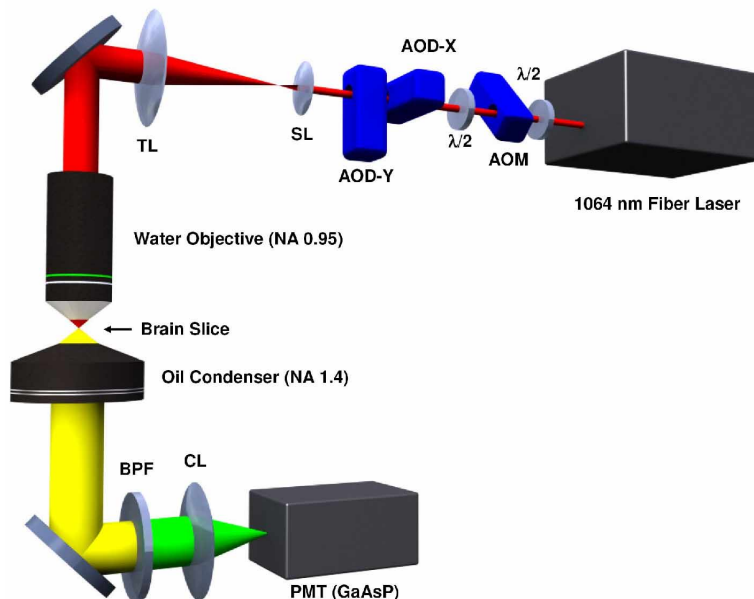

Fig. 1. Random access second-harmonic generation (RASH) microscope. A fiber laser provided the excitation light, which comprised 200 fs width pulses at 80 MHz repetition rate. The laser beam was adjusted for optimal linear polarization via a half-wave (λ/2) plate. Beam passes were made through 45° AOM for angular spreading pre-compensation. A second half-wave (λ/2) plate was placed after the AOM to optimize the diffraction efficiencies of the 2 orthogonally mounted AODs (AOD-x and AOD-y). A scanning lens (SL) and a microscope tube lens (TL) expanded the beam before it was focused onto the specimen by the objective lens. The SHG signal was collected by an oil immersion condenser, band-pass filtered (BFP) and focalized by a collection lens (CL) into a GaAsP PMT.

During the optical recording of Vm the line scans were oriented parallel to the soma membrane to increase the S/N. By intensity plot profiles of the line scan signal we estimated that only the 10 % of the collected signal during the scanning procedure is derived from the surrounding neuropil.

2.4 Analysis

The electrophysiology traces were analyzed using Origin 7.5 (Microcal Software). The optical data were analyzed with software written in LabVIEW 7.1 (National Instruments). The neuropil signal was removed in the analysis process. A Vm-independent bleaching effect during line scanning was corrected by fitting the signal baseline with a biexponential function. The probability of false events was calculated considering that the noise in the SHG signal is Poisson distributed. In our experimental conditions, the expected number of occurrences that

occur during a given interval is sufficiently large to approximate the noise in the SHG signal, which follows a Gaussian distribution. Under this hypothesis, and considering the non-correlated nature of shot noise, we can estimate the probability of one point overcoming an arbitrary threshold as the integral of a normalized Gaussian distribution from the threshold value to ∞. The validity of this calculation was verified in experimental SHG traces where electrical activity was not present.

3. Results

3.1 Staining and imaging

Acute cerebellar slices were cut from the vermis on the parasagittal plane according to standard techniques [24] and were labeled by bulk loading of the dye FM4-64 (see Fig. 2(a) and 2(b)). As reported in Fig. 2(c) and 2(d), the staining procedure did not have any influence on the electrophysiological properties of PCs in the slice [25,26]. Both in unstained (n = 8) and stained (n = 8) conditions, cells showed the typical autorhythmic activity and no statistically significant differences were measured in the input resistance, AP duration, firing threshold and AP amplitude (see Table 1).

Table 1. Electrophysiological properties of PCs. Input resistance, AP duration, firing threshold and AP amplitude between the stained (n = 8) and unstained (n = 8) slices. The AP amplitude was measured respect to the firing threshold. The numbers represent mean ± standard deviation.

	Unstained slice	Stained slice
Input resistance (MΩ)	57 ± 13	55 ± 8
AP duration (ms)	0.9 ± 0.1	0.8 ± 0.1
Firing threshold (mV)	-46 ± 7	-40 ± 4
AP amplitude (mV)	73 ± 5	66 ± 4

To test the effective nature of the action potentials recorded in PCs, the climbing fibers were stimulated while intracellularly injecting a negative holding current with different intensities. Figure 2(e) shows the response of the PC to the same stimulus starting from different membrane potentials. It should be noted that when the cell is silenced from its autorhythmic activity and stimulated with a single stimulus, the response has the typical shape of a complex spike. Moreover by increasing the hyperpolarizing current, the number of spikelets progressively decreased. The complex spikes show the same typical shape in both unstained and stained slices.

Figure 2(f) shows SHG images of the granule, Purkinje and molecular layer in a sagittal slice of the cerebellar cortex at three different penetration depths. The identification of the cell types was performed by a comparison of bright field and second-harmonic generation images. At superficial depths (10 µm), strong signals were observed from the granule cells (yellow arrow), PCs (red arrow) and molecular layer interneurons (blue arrow). At depths greater than 50 µm, the signal from the granule cells was strongly attenuated, while the PCs could be visualized throughout the entire depth of the slice. In order to determine whether the attenuation of the signal in the granular layer was due to insufficient diffusion of the dye, we performed pressure injection [17] to deliver FM4-64 to the centre of the slice depth. Under these conditions, we observed identical results as seen in the bulk loading of the indicator: strong signals from PCs could be recorded at depths beyond 50 µm, however we observed a marked attenuation of signals from granule cells. We reasoned that the SHG signal from deep granule cells might cancel out [27] due to the tight packing of granule cells resulting in a symmetric distribution of the dye [28]. This hypothesis was confirmed by a comparison of the two-photon and second-harmonic images. We found the two-photon signal from granule cells is present also at depths beyond 50 µm while the second-harmonic signal disappears (data not

shown). Following this hypothesis, one should conclude that the distance between loaded neurons is greater in superficial layers than deeper in the slice, perhaps reflecting extracellular matrix relaxation. The bulk loading of FM4-64 was chosen for all further investigations because it was equivalent to pressure injection, yet less invasive and more useful in providing staining throughout the slice. All further experiments were performed on PCs at depths between 50 µm and 150 µm. In cultured cells, the ratio of the SHG signal collected from the membrane (M) to the external (E) or intracellular (I) compartment is extremely high (M/E ≈ M/I ≈ 10). In slices, the membrane specificity of the SHG signal was lower (M/I ≈ 5, M/E ≈ 3), but this fact does not influence the sensitivity of the SHG signal ($\Delta S/S$, defined for ΔVm of 100 mV) in reporting transmembrane potential (see below).
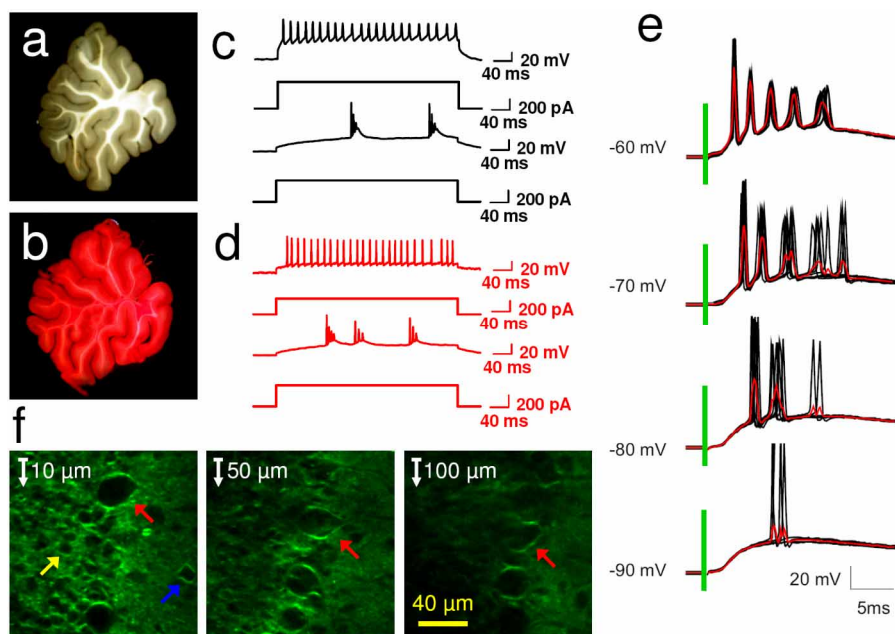

Fig. 2. Staining and imaging. a) A photograph of a sagittal cerebellar slice unstained, b) Cerebellar slice after incubation with FM4-64 (100 µg/ml) showing the dye loading throughout the tissue. c, d) Upper traces show sodium spikes typically recorded in the PC soma after current injection. Lower traces show calcium spikes coming from the dendritic compartment of the PC. These current clamp recording show normal physiological conditions in the unstained (c) and stained (d) condition. In these measurements, PCs were hyperpolarized at a holding potential of -70 mV. e) The four panels show traces of voltage transient (black line) in a single PC following stimulation of climbing fibers (green line) at different holding potentials (-60, -70, -80, -90 mV). For each holding potential, 20 sequential trials are shown superimposed. Red trace shows the average of the 20 trials. f) SHG image of cerebellar slice at three different depths of 10, 50 and 100 µm, oriented with the granule cell layer on the left and the molecular layer on the right. Examples of SHG signals from a PC (red arrow), granule cell (yellow arrow) and interneuron (blue arrow). The images were acquired with the same laser power across all three depths.

3.2 RASH optimization: signal to noise and photodamage

To reach our objective of using SHG for multi-unit recordings, we first optimized the RASH parameters (i.e. laser power, number of neurons simultaneously monitored and integration time per neuron). Figure 2(f) shows that the maximum field of view of our RASH microscope covers up to 5 PCs. On the other hand, recording of APs requires a sampling frequency of at least 2 KHz. These parameters set the maximum signal integration time per membrane pass to 100µs (including the 4 µs commutation time of the AODs). With this integration time, in

cultured neurons it was demonstrated that the laser power required to obtain a S/N of 4-5 (sufficient for recording APs in single trial) was below photodamage threshold [16]. The sample of interest in RASH microscopy, however, has profound physiological differences (eg. free oxygen concentration) with respect to cultured neurons, thus requiring a new exploration of the photodamage threshold during AP recording. The SHG signal from the somatic membrane was integrated over 100 µs, sampled at 2 kHz for a recording time of 50 ms. The laser power was then adjusted to obtain a S/N of 4-5. Unfortunately, in the majority of cases (≈ 80%, n = 10) a S/N of 4-5 could be obtained only at the expense of significant photodamage, as judged from decline of holding potentials and/or reduction of AP amplitude (measured by a patch-clamp electrode in whole cell configuration). For optimal application of RASH microscopy, we required that no measurable photodamage would occur, even under repetitive measurements. Lowering the laser power until this condition was fulfilled (n = 20) resulted in S/N ≈ 2 which, in turn, imposes averaging across repeated trials.

RASH microscopy can also be applied for measurements requiring single trial recordings, provided that the number of neurons monitored is reduced and the integration time per membrane pass is accordingly increased to obtain an adequate S/N. For example, we demonstrate below the possibility of single trial simultaneous recording on two neurons.

3.3 Optical single- and multi-unit recording of stimulated electrical activity

We stimulated climbing fibers to evoke the typical complex spike activity in PC (see Fig. 2(e)), while we simultaneously recorded SHG and electrical signals from the neuronal soma of one cell by single-line scan imaging and whole cell recording, respectively.
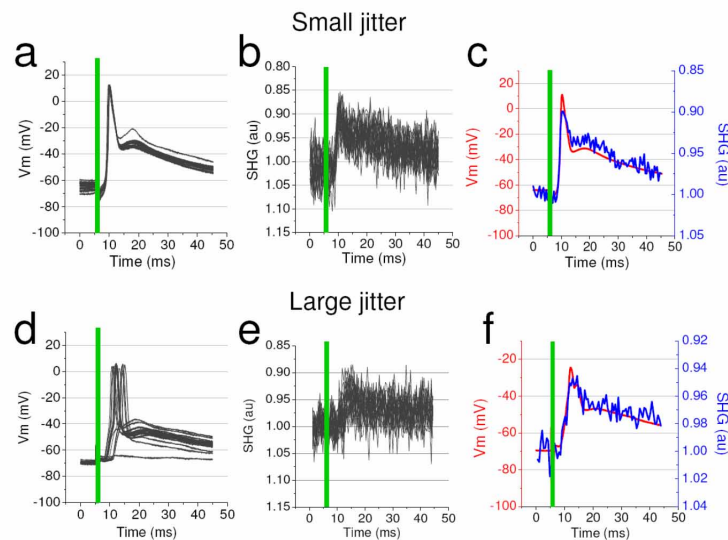

Fig. 3. Optical recording of APs induced by afferent fibers stimulation. a) Traces of APs in a single PC following stimulation of climbing fibers (green line). 20 trials are shown superimposed. b) Simultaneous SHG recording of APs in 20 trials, corresponding to the electrophysiological trace in a). Integration time 100 µs, sampling frequency 2 kHz. c) The average of the 20 trials are presented for both electrical (red trace) and SHG (blue trace) signals, showing how well the SHG changes track the membrane potential. d) Electrical traces of 20 trials demonstrating jitter in the response of PCs to the afferent stimulation. e) Simultaneous recording of SHG in 20 trials showing the commensurate jitter in the optical recordings. Integration time 100 µs, sampling frequency 2 kHz. f) Averaged traces of both electrical and SHG signals, showing the effect of jitter on broadening and attenuation of APs when multiple trials are averaged. In these measurements, PCs were hyperpolarized at a holding potential of -70 mV. One second was allowed between the 20 individual multi-line scans.

Electrical and optical recordings of a typical PC's AP are shown in Fig. 3. Each of the 20 trials is shown superimposed for the electrical (Fig. 3(a)) and optical (Fig. 3(b)) traces. Figure 3(c) shows the average of 20 trials for both the electrical and optical recordings. This Fig. clearly shows that the SHG signal follows the ΔVm with high fidelity in both the fast and slow time scales of the AP. A variation of $\approx$ 85 mV in membrane potential was associated with a ΔSHG/SHG of $\approx$ 10%, providing a ΔS/S $\approx$ 12%. This value is in good agreement with previous measurements in cultured cells and brain slices [16-18]. By averaging 20 consecutive scans, the SHG S/N was in the order of 10 (single trial delivering an S/N ratio $\approx$ 2), collecting $\approx$ 5 SHG photons per μs while scanning a given section of membrane. As discussed above, these scanning parameters produced no photodamage, based on the stable holding potential, amplitude and duration of the AP throughout the laser irradiation (see Fig. 3(a) and Fig. 3(d)).

In most of the experiments, we observed variability in the delay between the stimulation of the afferent fibers and the generation of the somatic AP (see Fig. 3(d)). This jitter is due to the varying integration time of synaptic responses, and allowed us to discard registrations with short latency indicating that somatic APs were generated by an antidromic stimulation of the axon. The jitter across trials causes a broadening of the measured AP and reduction in amplitude in the averaged trace. The averaged SHG signal also shows evidence of this jitter, which leads to an attenuation of the ΔSHG/SHG. An example of the effect of jitter is shown in Fig. 3(d), 3(e) and 3(f), where an average change in membrane potential of $\approx$ 45 mV was associated with ΔSHG/SHG of $\approx$ 5%. Despite the influence of jitter on the ΔSHG/SHG, there was no change in the ΔS/S, which remained $\approx$ 11%. The effect of jitter is also inherent in the multi-neuronal recordings (described below) and is one of the sources of the small attenuation in the amplitude of APs averaged across trials.

RASH microscopy was used to record membrane potential from multiple PCs with near simultaneous sampling. The RASH system AODs rapidly scanned between lines drawn in the membranes of neurons to perform multiplex measurements of the SHG signal. Figure 4(a) shows a field of view including 5 PCs at a depth of 90 μm.
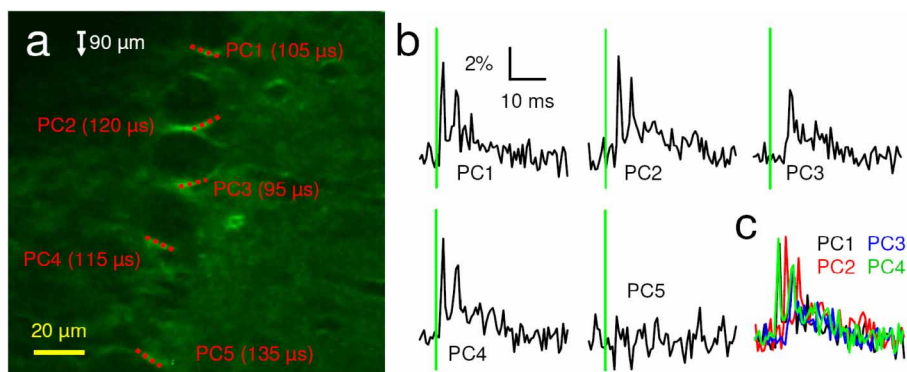

Fig. 4. Optical multi-unit recording of stimulated electrical activity. a) SHG image of a cerebellar slice taken at a depth of 90 μm. The multi-unit SHG recording was carried out from the lines drawn (dotted red) on the 5 PCs, with the integration time per membrane pass indicated. b) Multiplexed recording of APs from the 5 PCs following stimulation of climbing fibers (green lines). Each trace represents the average of 20 trials for each PCs. The time resolution is 0.47 ms. c) Superposition of SHG traces corrected for multiplex delay is shown. PC5 is not shown since it was quiescent.

The lines drawn through the membrane of each neuron and the signal integration time per membrane pass are indicated beside each cell in Fig. 4(a). Individual raw SHG traces are shown in Fig. 4(b) and real-time traces were corrected for multiplexing delay, as summarized in Fig. 4(c). Complex spikes were observed in PCs and evidence of synchrony and asynchrony was observed across the population of neurons. PC5 in Fig. 4(b) was not active

across trials, where the membrane SHG at baseline signal would have been sufficient to detect an AP. Assuming that all cells are viable, this quiescence could be due to multiple reasons, including low release probability leading to the generation of few and jittered spikes, or stimulation of a set of fibers not directly connected with this PC, since it has been shown that each climbing fiber branches into a final subset of fibers contacting on average 5 adjacent cells [29,30]. The results of Fig. 4 show that the averaging procedure is useful for studying triggered responses; however, the autorhythmic simple spike firing of PCs would be effectively cancelled-out by the process of averaging. In order to record spontaneous activity, APs must be detected in a single trial without averaging.

3.4 Optical multi-unit recording of spontaneous electrical activity

Maintaining a sampling frequency of 2 kHz, single trial AP recordings without photodamage could be achieved increasing the integration time per membrane pass to ~ 250 µs. With these parameters, spontaneous activity can be simultaneously monitored in two neurons. Figure 5 shows a spontaneous AP resolved without averaging in two PCs. The membrane integration time per neuron was ~ 250 µs. The electrical activity of one neuron was monitored by a patch-clamp electrode in loose cell attached configuration (PC1 in Fig. 5(a)).
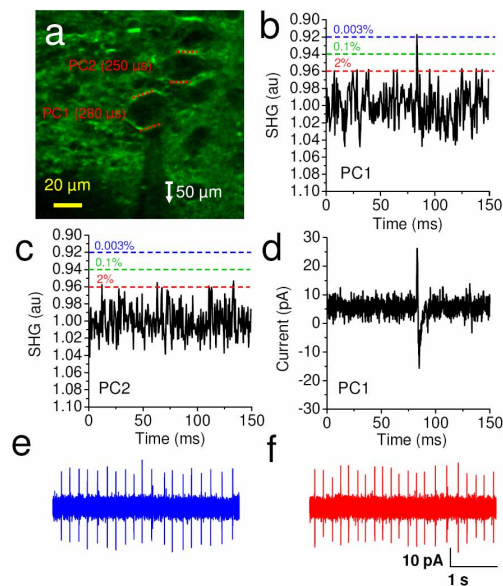

Fig. 5. Optical multi-unit recording of spontaneous electrical activity. a) SHG image from a cerebellar slice taken at a depth of 50 µm. The multi-unit SHG recording was carried out from the lines drawn (dotted red) on PC1 and PC2, with the integration time per membrane pass indicated. PC1 was also measured simultaneously by electrophysiology (shadow of electrode can be seen below PC1). b) SHG signal from PC1 showing a spontaneous AP recorded in a single trial. Each point represents 0.535 ms. Confidence intervals are drawn indicating the probability of the noise crossing thresholds. The probability of the noise crossing a threshold of 0.92 is 0.003%, indicating the event shown is an AP (see panel e). c) SHG signal from PC2, suggesting that no spontaneous activity was detected in this 150 ms sampling time. d) Simultaneous electrical recording of PC1, corresponding to the SHG trace shown in panel b. The electrical recording of spontaneous activity in PC1 before e) and after f) the SHG signal collection.

Figure 5(b) and 5(c) show the SHG signals from neurons PC1 and PC2, respectively. The simultaneous electrical recording of PC1 is shown in Fig. 5(d), where a single, spontaneous AP was observed. As reported in Fig. 5(b), this AP was also clearly observed in the SHG trace as a point significantly above the background noise. Given that the noise in the SHG signal is

Poisson distributed, we established the probability of one point overcoming an arbitrary threshold (see Materials and Methods), as shown in Fig. 5(b) and 5(c). Considering a $\Delta S/S \approx$ 10 %, a spontaneous AP should correspond to a $\Delta SHG/SHG \approx$ 6 - 8%. The probability of one point exceeding a threshold of 0.94 ($\Delta SHG/SHG = 6\%$) is 0.1% and, with a threshold set at 0.92 ($\Delta SHG/SHG = 8\%$), this estimate decreases to 0.003%. This means that the signal exceeding this threshold is an AP with a level of confidence of 99.997%, as indicated in Fig. 5(b). Setting a threshold for spike detection at a $\Delta SHG/SHG \approx 6\%$, therefore, permits the detection of spontaneous APs with a good level of confidence. Consequently, the SHG recording from PC2 shows evidence of quiescence during this sampling period, since the S/N would be sufficient to detect any APs. Furthermore, the experimental parameters used in this approach did not lead to photodamage, as shown by the similarity of spontaneous activity before (Fig. 5(e)) and after (Fig. 5(f)) the optical recording period.

4. Discussion

We have presented a novel optical method for recording multi-unit electrical activity in intact neuronal networks in brain slices. The bulk loading of FM4-64, combined with RASH microscopy, provides a fast and non-invasive approach to measure APs in neuronal assemblies.

Local network activity in PCs, in response to triggered stimulation, was successfully recorded by averaging across a series of trials. Although we have presented recordings of APs induced by afferent fiber stimulation in clusters of up to 5 neurons, this is by no means a limitation of the apparatus. For example, the number of neurons that could be recorded can be enhanced by decreasing the integration time of each membrane pass. To reach a comparable S/N, one must simply increase the number of trials to average. A sampling frequency comparable to conventional electrophysiology (~10 kHz) could easily be achieved by reducing the number of neurons simultaneously acquired and/or the integration time per membrane pass. The recording of APs in clusters of deep neurons achieved in this work has not been possible with previous techniques.

We have shown the near-simultaneous detection of spontaneous activity of two PCs in single trial recordings. Although at the moment the detection of spontaneous firing activity is limited to pairs of neurons, a task that can also be performed with double patch-clamp recordings, RASH microscopy allows more freedom in choosing neurons and rapidly switching between cells without changing and repositioning electrodes. Presently, the main limitation of RASH microscopy is photodamage. Because the SHG signal voltage response is small, high illumination intensities and/or laser integration times must be used to attain useful S/N. The development of more efficient SHG probes [31] or laser excitation strategies to minimize photodamage [32] will permit this technique to be used to optically record spontaneous electrical activity in larger assemblies of neurons.

RASH microscopy is a very versatile and promising method complementary to existing electrophysiological techniques. For example, multi-electrode arrays (MEA) can measure the single unit activity from large populations of neurons (e.g. PC in cerebellar cortex [24,33]), but the electrodes are placed in fixed positions and spaced by distances usually larger than 50 µm. This constraint can be overcome by RASH microscopy, which can detect the activity of adjacent neurons located at any position in a chosen field of view. Whilst this field of view may be sufficient to investigate characteristics of local networks, a combination of RASH microscopy and MEA techniques would provide a more complete description of global network dynamics.

Although the 2-D RA excitation scheme used here was appropriate for the well defined planar geometry of the cerebellum, RASH microscopy could easily be implemented with a 3D RA scanning system [34] to record the electrical activity of more complex, multidimensional networks in intact brain slices.

There is also a significant potential to combine RASH microscopy with laser stimulation methods to determine the connectivity of neuronal networks. For example, the approach of

using patterned laser uncaging of neurotransmitters [35] or two-photon stimulation of neurons [36] would be ideal complements to multi-unit recording with RASH microscopy. Similarly, the optical control of neural activity with opsin-based genetic tools [37], would be an excellent application with RASH to rapidly interrogate the connectivity of neuronal circuitry.

Acknowledgments